Research Article | Vol. 25, No. 20 | 2 Oct 2017 | OPTICS EXPRESS 23873
Optics EXPRESS

Graphene-assisted high-efficiency liquid crystal tunable terahertz metamaterial absorber

LEI WANG,[1,2,3,*] SHIJUN GE,[2] WEI HU,[2] MAKOTO NAKAJIMA,[3] AND YANQING LU[2]

[1]*School of Optoelectronic Engineering, Nanjing University of Posts and Telecommunications, Nanjing 210023, China*
[2]*National Laboratory of Solid State Microstructures, Collaborative Innovation Center of Advanced Microstructures and College of Engineering and Applied Sciences, Nanjing University, Nanjing 210093, China*
[3]*Institute of Laser Engineering, Osaka University, Suita, Osaka 565-0871, Japan*
[*]*wangl@njupt.edu.cn*

Abstract: In this paper, few-layer porous graphene is integrated onto the surface of a metasurface layer to provide a uniform static electric field to efficiently control liquid crystal, thereby enabling flexible metamaterial designs. We demonstrate a tunable cross-shaped metamaterial absorber with different arm lengths driven by this combined metasurface and graphene electrode. The resulting absorber supports a resonant frequency tunable from 0.75 to 1 THz with a high-quality factor, and amplitude modulation of ~80% at these frequencies with an applied voltage of 10 V. Furthermore, the near-field intensity and hot spot distribution can be manipulated over a broad range.

OCIS codes: (300.6495) Spectroscopy, terahertz; (230.3720) Liquid-crystal devices; (160.3918) Metamaterials.

References and links

1. B. Ferguson and X.-C. Zhang, "Materials for terahertz science and technology," Nat. Mater. **1**(1), 26–33 (2002).
2. M. Tonouchi, "Cutting-edge terahertz technology," Nat. Photonics **1**(2), 97–105 (2007).
3. M. Hangyo, "Development and future prospects of terahertz technology," Jpn. J. Appl. Phys. **54**(12), 120101 (2015).
4. S. Savo, D. Shrekenhamer, and W. J. Padilla, "Liquid Crystal Metamaterial Absorber Spatial Light Modulator for THz Applications," Adv. Opt. Mater. **2**(3), 275–279 (2014).
5. Y. Tadokoro, T. Nishikawa, B. Kang, K. Takano, M. Hangyo, and M. Nakajima, "Measurement of beam profiles by terahertz sensor card with cholesteric liquid crystals," Opt. Lett. **40**(19), 4456–4459 (2015).
6. D. Shrekenhamer, W. C. Chen, and W. J. Padilla, "Liquid Crystal Tunable Metamaterial Absorber," Phys. Rev. Lett. **110**(17), 177403 (2013).
7. D. C. Zografopoulos and R. Beccherelli, "Tunable terahertz fishnet metamaterials based on thin nematic liquid crystal layers for fast switching," Sci. Rep. **5**(1), 13137 (2015).
8. C. C. Chen, W. F. Chiang, M. C. Tsai, S. A. Jiang, T. H. Chang, S. H. Wang, and C. Y. Huang, "Continuously tunable and fast-response terahertz metamaterials using in-plane-switching dual-frequency liquid crystal cells," Opt. Lett. **40**(9), 2021–2024 (2015).
9. N. Chikhi, M. Lisitskiy, G. Papari, V. Tkachenko, and A. Andreone, "A hybrid tunable THz metadevice using a high birefringence liquid crystal," Sci. Rep. **6**(1), 34536 (2016).
10. B. Vasić, D. C. Zografopoulos, G. Isić, R. Beccherelli, and R. Gajić, "Electrically tunable terahertz polarization converter based on overcoupled metal-isolator-metal metamaterials infiltrated with liquid crystals," Nanotechnology **28**(12), 124002 (2017).
11. Z. B. Ge, S. T. Wu, S. S. Kim, J. W. Park, and S. H. Lee, "Thin cell fringe-field-switching liquid crystal display with a chiral dopant," Appl. Phys. Lett. **92**(18), 181109 (2008).
12. X.-W. Lin, J.-B. Wu, W. Hu, Z.-G. Zheng, Z.-J. Wu, G. Zhu, F. Xu, B.-B. Jin, and Y.-Q. Lu, "Self-polarizing terahertz liquid crystal phase shifter," AIP Adv. **1**(3), 032133 (2011).
13. C. S. Yang, T. T. Tang, P. H. Chen, R.-P. Pan, P. Yu, and C.-L. Pan, "Voltage-controlled liquid-crystal terahertz phase shifter with indium-tin-oxide nanowhiskers as transparent electrodes," Opt. Lett. **39**(8), 2511–2513 (2014).
14. Y. Wu, X. Ruan, C.-H. Chen, Y. J. Shin, Y. Lee, J. Niu, J. Liu, Y. Chen, K.-L. Yang, X. Zhang, J.-H. Ahn, and H. Yang, "Graphene/liquid crystal based terahertz phase shifters," Opt. Express **21**(18), 21395–21402 (2013).
15. L. Wang, X. W. Lin, W. Hu, G. H. Shao, P. Chen, L. J. Liang, B. B. Jin, P. H. Wu, H. Qian, Y. N. Lu, X. Liang, Z. G. Zheng, and Y. Q. Lu, "Broadband tunable liquid crystal terahertz waveplates driven with porous graphene electrodes," Light Sci. Appl. **4**(2), e253 (2015).

#296995 https://doi.org/10.1364/OE.25.023873
Journal © 2017 Received 31 May 2017; revised 14 Sep 2017; accepted 17 Sep 2017; published 20 Sep 2017

Optics EXPRESS

16. H. T. Chen, "Interference theory of metamaterial perfect absorbers," Opt. Express **20**(7), 7165–7172 (2012).
17. L. Q. Cong, S. Tan, R. Yahiaoui, F. P. Yan, W. L. Zhang, and R. Singh, "Experimental demonstration of ultrasensitive sensing with terahertz metamaterial absorbers: A comparison with the metasurfaces," Appl. Phys. Lett. **106**(3), 031107 (2015).
18. L. Wang, S. J. Ge, Z. X. Chen, W. Hu, and Y. Q. Lu, "Bridging the terahertz near-field and far-field observations of liquid crystal based metamaterial absorbers," Chin. Phys. B **25**(9), 094222 (2016).
19. L. Wang, X. W. Lin, X. Liang, J. B. Wu, W. Hu, Z. G. Zheng, B. B. Jin, Y. Q. Qin, and Y. Q. Lu, "Large birefringence liquid crystal material in terahertz range," Opt. Mater. Express **2**(10), 1314–1319 (2012).
20. M. Schadt, H. Seiberle, and A. Schuster, "Optical patterning of multi-domain liquid-crystal displays with wide viewing angles," Nature **381**(6579), 212–215 (1996).
21. S. Slussarenko, A. Murauski, T. Du, V. Chigrinov, L. Marrucci, and E. Santamato, "Tunable liquid crystal q-plates with arbitrary topological charge," Opt. Express **19**(5), 4085–4090 (2011).
22. B. Y. Wei, W. Hu, Y. Ming, F. Xu, S. Rubin, J. G. Wang, V. Chigrinov, and Y. Q. Lu, "Generating switchable and reconfigurable optical vortices via photopatterning of liquid crystals," Adv. Mater. **26**(10), 1590–1595 (2014).

1. Introduction

With recent rapid developments in terahertz (THz) technology, THz radiation has been used in applications as diverse as security screening, biological medical, and high-speed wireless communication [1–3]. THz absorbers, which are critical components in THz detectors, imagers, and sensors, are in high demand [4,5] and designers now expect tunability and higher performance. Liquid crystal (LC) based THz metamaterial absorbers (TMAs) promise to deliver the required performance, not only because LC-based display technology is mature, but TMAs can enhance the THz near-field while operating as an electrode to control a few microns-thick LC with an external electric field. The response of tunable TMAs is orders of magnitude faster than that of LC-based non-resonant terahertz components. Several previous works have explored LC-based tunable TMAs with different metamaterial patterns. The first LC tunable metamaterial absorber in the THz regime was demonstrated by Padilla et al. in 2013 [6]. In 2015, a tunable THz fishnet metamaterial based on a thin LC layer for fast switching and tunable THz metamaterials using in-plane electrodes were reported [7,8]. Then, a hybrid tunable THz metadevice using a high birefringence LC was proposed in 2016 [9]. Recently, an electrically tunable THz polarization converter based on over-coupled metamaterials infiltrated with an LC was invented by Vasić et al. [10].

The structure of existing LC tunable TMAs must support convenient connections to electric power sources in order to apply the necessary voltage to control the LC. The adjacent units of a metasurface layer, such as a fishnet or grating, are connected to each other in at least one direction. However, the connecting wires may cause low quality (Q) factors and polarization sensitivity, which are undesirable. Thus, the options are limited for designing high-performance TMAs. In addition, metasurfaces used as electrodes only supply a nonuniform static electric field, especially in thin LC layers, and this does not allow efficient control of the LCs due to the fringe field effect [11], unless a very high voltage is applied. Consequently, the maximum obtainable tunability of TMAs in both far-field and near-field is small, which has significantly limited their application. Conventional non-resonant LC THz devices have a simple construction with a uniform static electric field [12,13]. But their response time is slow due to the thick cell gap, which make these types of devices impractical. If high-performance metamaterials can be used to supply a uniform static electric field to an LC, it may be possible to further improve the efficiency and tunable range.

Graphene is a promising candidate for transparent electrodes in the THz regime, such as indium tin oxide (ITO) in the visible band, which are essential for LC-based THz tunable devices [14]. However, the electrical resistance and transparency of graphene in the THz band are not as good as those of ITO in the optical range. Although few layer graphene can be used to improve the resistance, the transparency becomes worse. To address these issues, we developed few-layer porous graphene (FLPG) through the UV/ozone method (VUO) that has randomly distributed micro scale hollows. FLPG is employed as an electrode due to its transmittance of more than 98% while reducing the resistance [15]. However, the graphene

Optics EXPRESS

film still has seven times the resistance of ITO and can only supply a uniform static electric field to control the LC without THz enhancement. Combining the graphene with a metasurface not only extends the design flexibility of the metamaterial with high Q but also reduces the resistance of the electrode.

Here, we produce a high-efficiency composite electrode by integrating a metasurface with FLPG, which is easy to process. We demonstrate an LC widely tunable THz metamaterial absorber not only in the far-field but also in the near-field based on the integrated electrode with low operating voltage. The absorber consists of a cross-shaped metasurface with different arm lengths, which has a reasonably high Q. Each unit of the metasurface is connected by the FLPG, and in turn, the resistance of the FLPG is improved by the unit. There are many potential applications for this novel absorber.

2. Schematic and principle

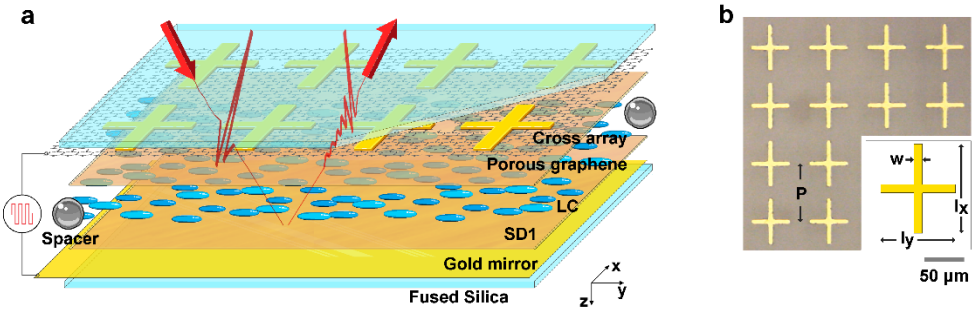

Fig. 1. Liquid crystal tunable metamaterial/graphene absorber: (a) schematic, and (b) optical image of the metasurface (inset: a unit cell of the metasurface), P = 150 μm, l_x = 120 μm, l_y = 100 μm, w = 10 μm.

Figure 1(a) shows the structure of the graphene-assisted LC tunable terahertz metamaterial absorber. It mainly consists of a metasurface, LC dielectric layer, and metal ground plane. The metasurface layer is made of a cross-shaped resonator with different arm lengths, as shown in Fig. 1(b). The periodicity is 150 μm and the arm lengths are 120 μm and 100 μm, respectively, with a width of 10 μm, as shown in the inset of Fig. 1(b). Both the top metasurface and bottom ground plane layers are 200-nm-thick Au which cover on fused silica substrates respectively. The FLPG is transferred onto the cross-shaped structure. Both of the metasurface/graphene upper electrode and metal ground electrode are spin-coated with sulfonic azo dye (SD1) as the alignment layers. The homogeneous alignment of a high-birefringence LC is implemented on the electrodes via a non-contact photo-alignment technique. The two substrates are assembled using epoxy glue and uniformly separated by 15 μm sphere-shaped silica spacers to form a cell which was infiltrated with LCs. The thickness of the LC layer is about 15 μm, and the optical axis of the LC is initially parallel to the y-axis. The absorber is driven by applying a 1 kHz square-wave alternating current signal through the copper tapes connecting the graphene and metal electrodes to the electric power source.

The working principle is the same as that of an ordinary LC tunable TMA [6,16]. The metasurface strongly couples to the incident THz electric field, and pairing the metasurface with a metal ground plane creates a mechanism for coupling to the magnetic component of the THz wave. Both the metal itself and the dielectric loss of the middle layer dissipate incident energy. The absorption (A) and reflectance (R) are related by A = 1 - R, and the transmittance (T) = 0 due to the metal ground plane. The FLPG applied to the metasurface as a transparent electrode has no effect on the features of the TMA, which facilitates a structure with a relative high Q [17]. We exploited a cross-shaped resonator with two different arm lengths to realize different resonant absorption frequencies. By altering the applied voltage between the metasurface/graphene and metal ground electrodes, we can efficiently tune the

Optics EXPRESS

refractive index of the middle LC layer, which allows for wide tunability of the resonant frequency and redistributes the THz enhancement spatial area with a low operating voltage.

3. Simulations

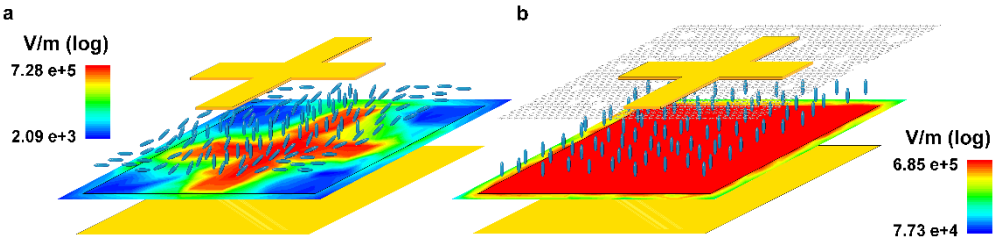

Fig. 2. Simulations of the static electric field and LC director distributions shown at a plane centered in the LC layer when the operating voltage is 10 V: (a) cross-shaped electrode, and (b) metamaterial/graphene electrode with the same metal ground.

First, we simulated the static electric field produced by the different electrodes to demonstrate the distributions of the LC director. The middle cutplane of the LC layer was chosen for analysis. The electric field intensity scale is defined by a color bar. From Fig. 2(a), when only a cross-shaped metasurface was used as an electrode, there was an obvious fringe field effect at 10 V where the strong electric field was focused on the cross-shaped area and the weak electric field was focused on the edge. Taking the small cell gap into account, the electric field over the entire LC layer was nonuniform, which led to an inhomogeneous LC director distribution. Only the LCs in the cross-shaped region re-oriented their directors vertically. The orientation of the directors gradually changed along with the electric field intensity. The LCs were slightly tilted near the rim where electric field intensity was zero. As the applied voltage increased, more LCs became vertically oriented, but the power consumption increased or even caused breakdown of the LC cell. To improve the efficiency of the overall device, we used a metamaterial/graphene electrode, which is similar to a parallel plate electrode, to produce a uniform electric field, as shown in Fig. 2(b). At 10 V, the electrode reached the saturated state and all the LC directors were re-oriented from planar to homeotropic. The simulation results indicate this hybrid electrode can supply a uniform electric field and induce a homogeneous rotation of the LC directors, which further confirms the operation of the proposed tunable TMA.

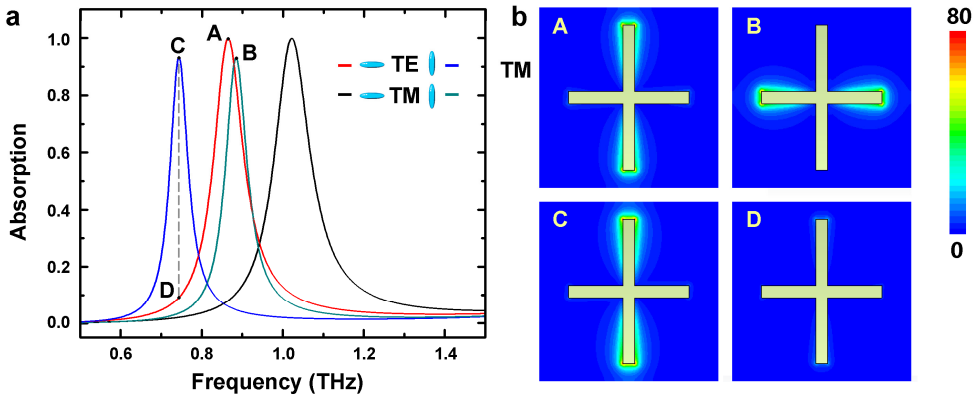

Fig. 3. Simulations of the tunability of the terahertz resonant frequencies and hot spots of the metamaterial absorber: (a) tunable absorption of TE and TM mode (b) electric field of the corresponding points in (a) at a plane 1 μm above the cross-shaped metasurface. A: 0.864 THz, 0 V, B: 0.884 THz, 10 V, C: 0.742 THz, 10 V, D: 0.742 THz, 0 V. The orientation of LC is horizontal at 0 V while vertical at 10 V.

Optics EXPRESS

We employed CST Microwave Studio to investigate the tunable range of the resonant frequency and the near field enhancement of the TMA. A perfect electric conductor (PEC) was used to simulate the metal, and the frequency dependent absorption was obtained from S-parameter simulations with periodic boundary conditions. Starting initially from the unbiased state where the LC was aligned parallel to the substrate with $n_o = 1.5 + j0.05$, because the polarization of THz electric field in the middle layer of the metamaterial absorber is mainly vertical [6,18], to the saturated state at 10 V where the LCs were aligned perpendicularly with $n_e = 1.8 + j0.03$ [19] due to our integrated electrode. The absorption peak frequencies had a redshift from 0.864 THz to 0.742 THz in transverse-electric (TE) mode (i.e., the electric field in the x-direction), and from 1.022 THz to 0.884 THz in transverse-magnetic (TM) mode (i.e., the electric field in the y-direction), as shown in Fig. 3(a). Due to the features of our metasurface, the resonance behavior exhibited a much superior Q factor in different frequency ranges as in Ref [17]. For example, the absorption had a full width half maximum of 0.1 THz at 0.9 THz (A) with a Q of approximately 10.

The reorientation of the LC director by increasing the applied voltages not only led to the strong modulation of the absorber resonance frequency and amplitude, but the redistribution of the hot spots in the near field of the TMA. We have studied the enhanced resonant fields in the spacer layer [18]. Here we take the enhancement above the absorber surface into account. A cutplane located 1 μm above the cross-shaped metasurface was chosen to explore the electric field redistribution induced by the LC rotation. As observed in Fig. 3(b), the THz electric field was concentrated at the ends of the cross in accordance with the previous results [16,17]. Note that when the LC was tuned from 0 V to 10 V, the corresponding orientation of LC from horizontal to vertical, there was a phenomenal shift in the electric field enhancement from one arm (A) to the other (B) while the resonant frequency was almost the same at approximately 0.874 THz. The enhanced electric field area and hot spot size in the same arm (C) became slightly larger with an absorption frequency of 0.742 THz. The intensity of the nonresonant electric field at this frequency in the unbiased situation became very weak (D). The electric field resonant enhancement in the LC layer as well as above the surface of the absorber originated from the multiple reflections between the top and bottom electrodes, and played a significant role in the tunability of the THz resonant absorption, which has tremendous potential for modulation and sensing applications.

4. Experiments

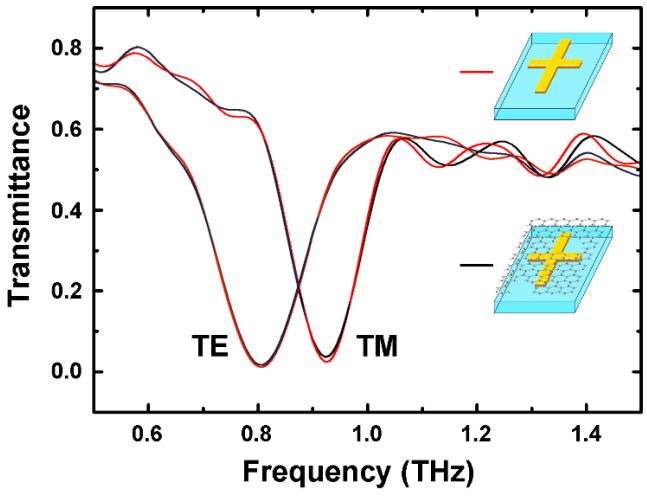

Fig. 4. Experimentally measured frequency- and polarization-dependent THz transmittances of the pristine, few-layer porous graphene coated cross-shaped electrode.

Optics EXPRESS

First, we fabricated the cross-shaped metasurface via photolithography and Au deposition with a thickness of approximately 200 nm onto 550-μm-thick fused silica. Then, the CVD-grown few-layer graphene was transferred onto the surface of the cross. The graphene film was UVO treated using a UV cleaning machine to introduce porous structures. Finally, the cell with the alignment layers was infiltrated with LC [20]. The NJU-LDn-4 LCs and fabrication methods were the same as those in our previous work [15]. The THz transmittances of the electrodes were measured using a THz time-domain spectroscopy (TDS) system (Advantest TAS7400SP) with a transmission analysis accessory. Figure 4 shows the frequency- and polarization-dependent spectra of the pristine, few-layer porous graphene coated cross-shaped metasurface. The resonant frequency of TE mode was about 0.81 THz while that in TM mode was about 0.92 THz. In the figure, the black curves represent the transmission spectra for the cross-shaped metasurface with the graphene covered, while the red curves show the results when the graphene was uncovered. The cross-shaped electrodes with and without FLPG had almost the same transmission spectra, which indicates the FLPG had no influence on the THz metamaterial. This means with only a few layers and limited porosity, the graphene was too slender to block the THz waves. On the other hand, considering the conductivity, the sheet resistance of the metamaterial/graphene film was measured to be ~400 Ω sq^{-1}, which is lower than that of the few-layer porous graphene itself [15]. Although it was not connected, the cross-structure between the substrate and graphene caused the electrode to be more conductive. The composite graphene/metamaterial electrode exhibited high-performance properties in both metamaterial and conductivity.

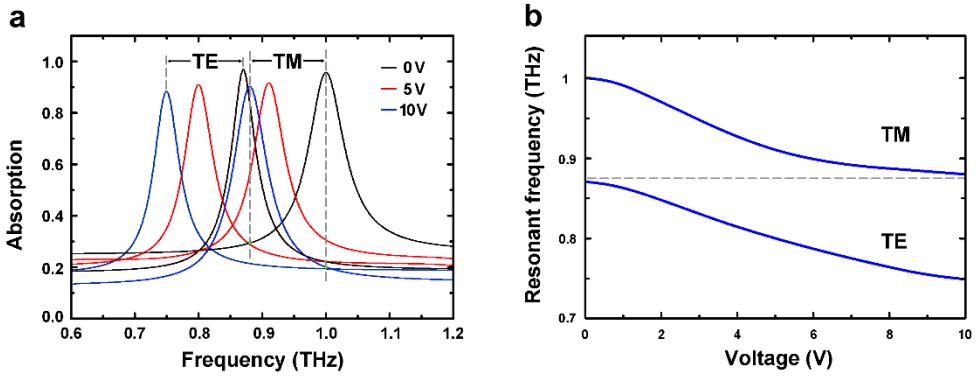

Fig. 5. Experimentally measured absorption response of the THz metamaterial absorber. (a) Frequency dependent absorption for different applied voltages. (b) Frequency location of the absorption maximum as a function of applied voltage.

Next, the absorption tunability of the graphene-assisted LC THz metamaterial absorber was characterized using the THz TDS system with reflection geometry. The reference was a same upper substrate as in our device with metal THz reflective plate covering on the top. The results are shown in Fig. 5 from which the influence of the upper substrate of our device was removed. Different voltages were applied to the absorber while the response was measured, as shown in Fig. 5(a). With no applied bias, we achieve an absorption of near 96% at 1 THz in TM mode, and 97% at 0.87 THz in TE mode, respectively. When the applied voltage increased to 5 V, strong corresponding redshifts at 80 GHz and 70 GHz occurred. At 10 V, the resonant absorptive feature shifted to 0.88 THz and 0.75 THz, both of which had a 120 GHz redshift. As amplitude modulation is desirable in many applications, we also considered the 1 THz operating frequency. When the applied voltage was 5 V, the absorption amplitude decreased to 30%, and was 20% when the applied voltage was 10 V. We realized an amplitude tuning of 80% at this resonant frequency.

Optics EXPRESS

A series of measurements were performed for different voltages. The voltage-dependent resonant frequency is presented in Fig. 5(b). As expected, both the TE mode and TM modes exhibited the same shift trend as the applied voltage increased. Generally, the resonant frequency decreased slowly below 1 V. As the voltage increased, it dropped quickly. Then at 10 V, it was near saturation. Consequently, the maximum tunable range could be from 1 THz to 0.88 THz for TM mode and from 0.87 to 0.75 THz for TE mode by tuning the applied voltage from 0 V to 10 V. Both the frequency range and amplitude tuning of the absorption peak of the metamaterial absorbers were realized. These results are consistent with the results of the theoretical analysis. The differences in the absorption amplitude between the simulation and experiment may have been caused by the loss of material.

Although we were limited to THz near field experiments, the redistributed enhanced electric field in the hot spot area was presented by way of simulation. By rotating the device or integrating it with the LC THz waveplate to change the polarization of the incident THz wave, we were able to tune the resonant frequency from 0.75 THz to 1 THz, which enables practical continuous single-frequency operation. When only a metasurface was used as an electrode to tune the LC, each unit must be connected, which places constraints on the metamaterial design. When a thin film of graphene is integrated as a transparent conductive material, high-performance flexible metamaterial devices can be constructed not only in the THz regime but also in other bands. The LC offers an extremely attractive avenue for fast-tuning the metamaterial enhanced electric field in the near-field and the resonant frequency in the far-field through the applied voltage.

5. Conclusions

By using the FLPG and metasurface as a combined electrode, we demonstrated a high-efficiency tunable THz absorber based on a large birefringence LC. The electrode combines the positive properties of both components. The graphene layer allows THz waves to propagate through and homogeneously tunes the LC material, while the metamaterial maintains its remarkable properties and improves the resistance of the FLPG. High tunability is realized in both the THz near and far fields with only a 10 V operating voltage. Graphene can be easily integrated into THz metamaterial devices, which permits designers to create any desired pattern for the metamaterial component. The proposed strategy provides a simple and promising path for the development of versatile tunable THz functional devices [21,22], such as THz spatial light modulators and array imagers, which will play important roles in THz imaging, sensing, and detection.

Funding

National Natural Science Foundation of China (NSFC) (No. 61605088); Natural Science Foundation of Jiangsu Province (No. BK20150845, 15KJB140004).

Acknowledgments

The authors are indebted to Prof. V. Chigrinov for his kind support with the photoalignment technique and thank Hao Qian for his assistance in drawing the schemes, and L. Wang also acknowledges financial support from the China Scholarship Council.